



Published in final edited form as:

J Virol Methods. 2021 November ; 297: 114196. doi:10.1016/j.jviromet.2021.114196.

A luciferase-based approach for measuring HBGA blockade antibody titers against human norovirus

Jessica M. van Loben Sels^{a,b}, Luke W. Meredith^a, Stanislav V. Sosnovtsev^b, Miranda de Graaf^c, Marion P.G. Koopmans^c, Lisa C. Lindesmith^d, Ralph S. Baric^d, Kim Y. Green^{b,*}, Ian G. Goodfellow^a

^aDivision of Virology, Department of Pathology, University of Cambridge, Cambridge, CB2 2QQ UK

^bCaliciviruses Section, Laboratory of Infectious Diseases, National Institute of Allergy and Infectious Diseases, National Institutes of Health, DHHS, Bethesda, MD, 20892 USA

^cDepartment of Viroscience, Erasmus University Medical Center, 3015 CN Rotterdam, NL

^dDepartment of Epidemiology, University of North Carolina, Chapel Hill, NC, 27599 USA

Abstract

Background: Noroviruses are the most common cause of viral gastroenteritis worldwide, yet there is a deficit in the understanding of protective immunity. Surrogate neutralization assays have been widely used that measure the ability of antibodies to block virus-like particle (VLP) binding to histo-blood group antigens (HBGAs). However, screening large sample sets against multiple antigens using the traditional HBGA blocking assay requires significant investment in terms of time, equipment, and technical expertise, largely associated with the generation of purified VLPs.

Methods: To address these issues, a luciferase immunoprecipitation system (LIPS) assay was modified to measure the norovirus-specific HBGA blockade activity of antibodies. The assay (designated LIPS-Blockade) was validated using a panel of well-characterized homotypic and heterotypic hyperimmune sera as well as strain-specific HBGA blocking monoclonal antibodies.

*Corresponding author at: Dr. Kim Y. Green, Caliciviruses Section, LID/DIR/NIAID, National Institutes of Health (NIH), Building 50, Room 6318, 50 South Drive, Bethesda, MD 20892 USA – kim.green@nih.gov.

Author Statement

Jessica M. van Loben Sels: Conceptualization, Investigation, Visualization, Writing-Original draft preparation. Luke W. Meredith: Investigation, Writing-Reviewing and Editing. Stanislav V. Sosnovtsev: Conceptualization, Investigation, Writing-Reviewing and Editing. Miranda de Graaf: Investigation, Resources, Funding Acquisition, Writing-Reviewing and Editing. Marion P.G. Koopmans: Investigation, Resources, Funding Acquisition, Writing-Reviewing and Editing. Lisa C. Lindesmith: Investigation, Resources, Writing-Reviewing and Editing. Ralph S. Baric: Resources, Investigation, Writing-Reviewing and Editing, Funding Acquisition. Kim Y. Green: Supervision, Funding Acquisition, Writing-Original draft preparation. Ian G. Goodfellow: Project administration, Conceptualization, Supervision, Funding Acquisition, Writing-Original draft preparation.

Conflicts of Interest

The authors declare no conflicts of interest.

Declaration of interests

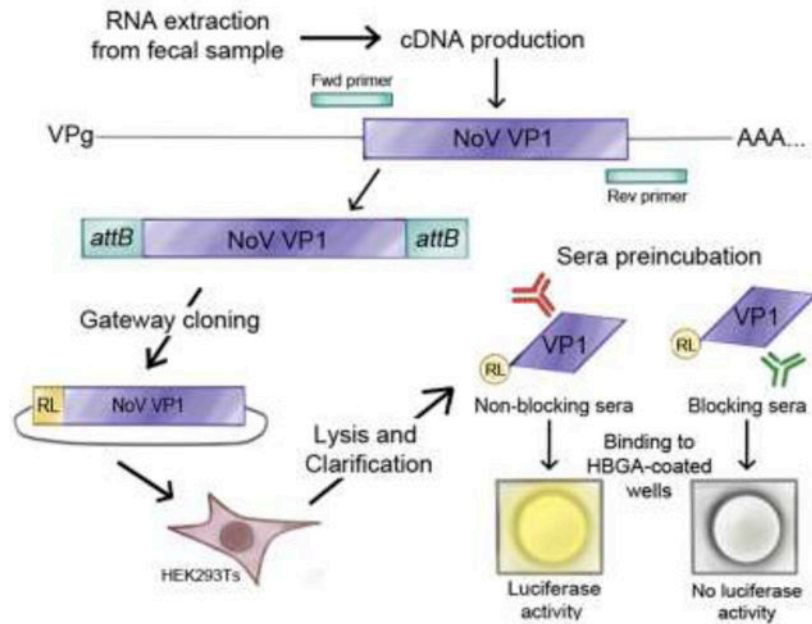
The authors declare that they have no known competing financial interests or personal relationships that could have appeared to influence the work reported in this paper.

Publisher's Disclaimer: This is a PDF file of an unedited manuscript that has been accepted for publication. As a service to our customers we are providing this early version of the manuscript. The manuscript will undergo copyediting, typesetting, and review of the resulting proof before it is published in its final form. Please note that during the production process errors may be discovered which could affect the content, and all legal disclaimers that apply to the journal pertain.

Results: The LIPS-Blockade assay was comparable in specificity to a standard HBGA blocking protocol performed with VLPs. Using time-ordered patient sera, the luciferase-based approach was also able to detect changes in HBGA blocking titers following viral challenge and natural infection with norovirus.

Conclusion: In this study we developed a rapid, robust, and scalable surrogate neutralization assay for noroviruses that circumvented the need for purified VLPs. This LIPS-Blockade assay should streamline the process of large-scale immunological studies, ultimately aiding in the characterization of protective immunity to human noroviruses.

Graphical abstract



Keywords

Human norovirus; LIPS assay; HBGA blockade assay; serology; VLPs

1. Introduction

Human noroviruses (HuNoVs) are the most common viral gastrointestinal pathogen in the human population, causing an estimated 200,000 deaths in children under the age of 5 in low-to-middle income countries (Patel, Widdowson et al. 2008, Iturriza-Gomara and O'Brien 2016). The wider societal impact and medical costs associated with HuNoV infections are an additional burden. In the United States, it is estimated that HuNoV-related hospital visits, diagnostics, and outpatient care cost about \$2 billion a year, a financial strain that could be alleviated with the availability of a vaccine (Bartsch, Lopman et al. 2012, Hoffmann, Batz et al. 2012, Bartsch, Lopman et al. 2016).

A member of the family *Caliciviridae*, HuNoVs are small, non-enveloped viruses with a single-strand, positive sense RNA genome approximately 7.7 kb in length. The genome of

HuNoV is divided into three open reading frames (ORFs) (Jiang, Wang et al. 1993). ORF1 encodes a nonstructural polyprotein that is cleaved into six proteins, including the viral RNA-dependent RNA polymerase (Hardy 2005). ORF2 encodes the major capsid protein, VP1, while a minor structural protein, VP2, is encoded by ORF3 (Glass, Zeng et al. 2003). The viral capsid is composed of 180 copies of VP1 which self-assemble into an icosahedral capsid. Vaccination with virus-like particles (VLPs) generated by expression of VP1 is sufficient to provide at least partial protection against infection (Atmar, Bernstein et al. 2011).

VP1 is divided into two domains - the shell (S) domain forms the internal structural core of the viral capsid, and the protruding (P) domain is exposed on the outermost surface. Noroviruses have been classified into ten genogroups based on differences in the VP1 sequence (Chhabra, de Graaf et al. 2019). Most HuNoV infections are caused by genogroups GI and GII, which are further subdivided into 9 and 27 genotypes, respectively. The majority of epidemic cases of HuNoV have been associated with GII.4, a genotype with high genetic diversity that gives rise to new, antigenically divergent strains about every 3–7 years (Lindesmith, Donaldson et al. 2011).

Until recent reports of permissive culture systems in B cells, zebrafish, and human enteroids (Jones, Grau et al. 2015, Ettayebi, Crawford et al. 2016, Van Dycke, Ny et al. 2019), there was no such system for human noroviruses. Protective antibodies have instead been characterized through a surrogate neutralization assay termed the HBGA blockade assay. This assay relies on the binding of virus-like particles (VLPs) to histo-blood group antigens (HBGAs), which contain carbohydrates that can be expressed on cell surfaces or secreted into bodily fluids. HBGA expression correlates with susceptibility to infection, as HBGAs are likely involved in viral attachment to permissive cells (Lindesmith, Moe et al. 2003). Based on vaccine studies, increases in antibody titers that block HuNoV binding to HBGAs correlate with increased protection against viral challenge (Reeck, Kavanagh et al. 2010, Lindesmith, Ferris et al. 2015, Ramani, Neill et al. 2017). Recent work with enteroids has demonstrated the correlation between HBGA blockade and neutralization of live virus infections *in vitro*, further demonstrating the useful predictive nature of the HBGA blockade assay (Atmar, Ettayebi et al. 2019, Lindesmith, McDaniel et al. 2019). A potential limiting factor in the use of the current HBGA blockade assay is its requirement for VLPs, which may not be readily available to a laboratory that does not have the infrastructure to produce them.

A luciferase immunoprecipitation system (LIPS) assay was recently developed for the detection of anti-HuNoV antibodies in sera (Tin, Yuan et al. 2017). Renilla luciferase-tagged VP1 antigens were used to determine antibody titers for a panel of HuNoV-immunized animal sera with accuracy comparable to that of a standard, VLP-based ELISA. The LIPS assay could profile the specificity of both strain-specific and cross-reactive sera, as well as detect changes in antibody titers following viral challenge. In this study, the LIPS assay was modified to create a luciferase-based method for evaluation of the titer and specificity of HBGA blocking antibodies, which are a functional subset of HuNoV-recognizing antibodies that have been associated with protective immunity. This assay circumvented the need for VLPs, providing a rapid and easily scalable method to increase the diversity of antigens used

to profile HBGA blockade antibodies. The ability to monitor the specificity and levels of protective immunity over time will facilitate the design of norovirus vaccines.

2. Materials and Methods

2.1 Cells and media

Insect cell lines SF9s and SF9-ETs were cultured in BaculoGROW insect cell medium (Oxford Expression Technologies), and Hi5 cells were cultured in EX-CELL 405 serum-free medium (Sigma Aldrich). Both media were supplemented with 10% heat-inactivated fetal bovine serum (FBS), 10 U/ml of penicillin, 100 µg/ml of streptomycin. Baculoviruses were amplified in suspension SF9 cells and titered on adherent SF9-ET cells (Hopkins and Esposito 2009). All insect cells were cultured at 28°C. HEK293Ts were cultured at 37°C in DMEM (Sigma Aldrich) supplemented with 10% heat-inactivated FBS, 10 U/ml of penicillin, 100 µg/ml of streptomycin and 2 mM L-glutamine (Sigma-Aldrich).

2.2 VLP production and purification

Suspension Hi5 insect cells were infected with baculoviruses engineered to express HuNoV VP1 at an MOI of 10 and incubated while shaking for 5 days at 28°C. Cells were lysed via three rounds of freeze-thawing, and cell debris was removed by centrifugation at 4000g for 30 minutes. Baculovirus was removed from the supernatant by centrifugation at 14000g for 30 minutes followed by 0.45-micron filtration. VLPs were precipitated by adding PEG-3350 10% w/v and stirring overnight at 4°C. Following two rounds of centrifugation at 27000g for 30 minutes at 4°C and resuspension of the pellet in boric acid buffer (0.2 M boric acid pH 7.5, 0.5 NaCl), the VLP-containing supernatant was purified over a 30% sucrose cushion in phosphate buffered saline (PBS) and spun at 150000g overnight at 4°C. VLP pellets were resuspended in boric acid buffer and mixed thoroughly with cesium chloride before being spun at 191000g for 20 hours. A visible band in the isopycnic cesium gradient, containing the VLPs, was removed by puncturing the tube with a needle, and the extracted layer was dialyzed in a 10,000 MWCO cassette against PBS overnight at 4°C. The concentrations of VLPs were determined via bicinchoninic acid (BCA) protein assay, aliquoted, and stored at -80°C. GII.4 MD145 baculovirus stocks were provided by Dr. Alexis de Rougemont. GII.4 Sydney2012 VLPs were produced as previously described (Lindesmith, Brewer-Jensen et al. 2017). VLP formation was confirmed by electron microscopy.

2.3 Construction of Rluc-VP1 fusion plasmids

ORF2 sequences from various HuNoV strains were amplified using primers that incorporated *attB1* sites upstream and downstream of the VP1 gene (underlined in Table 1). Following PCR, *attB1*-flanked VP1 genes were first cloned into the donor vector, pDONR207, and later the destination vector, pcDNA3.1-RL-GW, via Gateway cloning (construct provided by Pr. Jürgen Haas, University of Edinburgh). VP1-containing plasmids were confirmed using Sanger sequencing. Resulting constructs contained renilla luciferase fused to the N-terminus of HuNoV VP1 sequences and were designated Rluc-VP1.

2.4 Rluc-VP1 antigen production

HEK293T cells were transfected with each plasmid using Lipofectamine 2000 according to the manufacturer's protocol. A total of 10^6 cells per well were seeded in 6-well cell culture plates and transfected with $2\mu\text{g}/\text{mL}$ of Rluc-VP1 plasmid when the cell monolayer reached 95% confluency. In order to harvest the Rluc-VP1 fusion proteins, cells were lysed 24 hours post-transfection under conditions previously described (Tin, Yuan et al. 2017). Briefly, cells were lysed in lysis buffer A (50 mM Tris, pH 7.5, 100 mM NaCl, 5 mM MgCl_2 , 1% Triton X-100, 1X complete mini protease inhibitor cocktail). Crude lysates were clarified via centrifugation at $12000g$ and stored at -80°C . Rluc-VP1 lysates were thawed and kept on ice during all assays. Luciferase activity was confirmed by serially diluting clarified lysates and reading relative light output (RLU) in white 96-well plates on a GloMax luminometer (Promega; injection of $100\mu\text{L}$ native coelenterazine, diluted to $1\mu\text{g}/\text{mL}$ in PBS; two second delay between readings; five second integration time).

2.5 Western blot analysis

In order to confirm the expression of luciferase-tagged VP1 proteins, transfected HEK293Ts were washed with PBS and lysed 24 hours post-transfection with RIPA buffer. Protein concentrations of the lysates were determined by BCA protein assays, and appropriate amounts of lysate were added to sample loading buffer containing 10% β -mercapto-ethanol to equal a final concentration of $1\mu\text{g}/\text{mL}$. Samples were heated at 95°C for five minutes and separated on a 12.5% SDS-PAGE gel. The BioRad Trans-Blot Turbo system was used to transfer proteins onto a nitrocellulose membrane then blocked with 5% nonfat dry milk or BSA diluted in 1X PBS-0.05% Tween20 (PBS-T) for one hour at room temperature. Mouse anti-renilla luciferase polyclonal antibody (Millipore) and mouse anti-GAPDH polyclonal antibody (Protein Tech) were each diluted 1:1,000 in 5% nonfat dry milk or BSA in PBS-T. Anti-HuNoV strain-specific guinea pig serum was diluted 1:500. All probed membranes were incubated overnight at 4°C . Li-Cor secondary antibodies (IRDye 680CW donkey anti-rabbit IgG, IRDye 800CW goat anti-mouse IgG, and IRDye 800CW donkey anti-guinea pig IgG) were diluted 1:10,000 in 5% nonfat dry milk or BSA in PBS-T and incubated with their respective membranes for one hour at room temperature before being washed and developed using the Li-Cor Odyssey CLx imaging system.

2.6 Serological immunoassays

2.6.1 Ethics approval for animal and human sera—Ethics oversight for animal studies was conducted by the Animal Care and Use Committees of the NIH (guinea pigs and chimpanzees) or Pocono Rabbit Farm and Laboratory, Inc (rabbits) (Bok, Parra et al. 2011, Tin, Yuan et al. 2017). Human infection serum was collected with informed consent under a protocol approved by the IRB at the Erasmus MC medical ethical committee (MEC2013–082) (van Beek, de Graaf et al. 2016). Paired sera from a human norovirus GII.4 challenge study were obtained under an IRB-approved protocol (Frenck, Bernstein et al. 2012) and provided by Dr. Xi (Jason) Jiang at the Cincinnati Children's Hospital Medical Center, Cincinnati, Ohio.

2.6.2 Calculating equal VLP and Rluc-VP1 antigen input values—Determination of equal VLP and Rluc-VP1 input for ELISA and LIPS, respectively, were estimated as previously described (Tin, Yuan et al. 2017). For further confirmation, GI.1 NV VLPs of known concentrations were diluted in sodium bicarbonate buffer and used to coat clear Maxisorp plates in order to act as a standard. GI.1 NV Rluc-VP1 proteins from three separate preparations were diluted 1:10 in 90 μ L sodium bicarbonate buffer, assessed for RLU values, and used to coat wells adjacent to VLP standards in duplicate. Plates were incubated overnight at 4°C and blocked with 5% nonfat dry milk in PBS-T for one hour at room temperature. Plates were washed with PBS-T three times before adding a GI.1 NV-specific monoclonal antibody (Abcam) as the detecting antibody. Following three washes with PBS-T, anti-mouse HRP-conjugated antibodies (Sigma, diluted 1:1000 in PBS) were added and incubated for an hour at room temperature. Following four washes with PBS-T, 100 μ L of TMB substrate (Thermo Fisher Scientific) was added to each well and left to incubate at room temperature for 30 minutes before reading the absorbance at 651 nm. Negative control wells were coated with Rluc-JUN diluted 1:10 in sodium bicarbonate buffer.

VLP standards resulted in O.D. readings which were fit with linear regression models. O.D. readings from Rluc-VP1 wells were averaged and input into the standards' linear functions (GraphPad Prism) to estimate the comparable concentration of VP1 present in the Rluc-VP1 lysates. A final linear regression model was fit as a function of RLUs present in the GI.1 NV Rluc-VP1 lysates vs. calculated concentration of VP1. An input of 1 μ g VLPs was estimated to be equivalent to 1.8×10^6 RLUs in Rluc-VP1 lysate (Supplementary Figure 1).

2.6.3 LIPS assays and ELISA titrations—For LIPS titrations, Rluc-VP1 lysates were diluted to 2×10^6 RLU/mL in blocking buffer. Serum samples were serially diluted 4-fold in a 96-well format. A 100 μ L volume of normalized Rluc-VP1 lysate was added to 100 μ L of each serum dilution and incubated at 4°C for one hour in 96-well vinyl U-bottom plates. Then, 100 μ L aliquots of these antigen-antibody mixtures were added to duplicate wells of white protein A/G-coated plates (Thermo Scientific). After one hour of room temperature incubation, unbound Rluc-VP1 antigen was removed following three washes with PBS-T. Antibody-antigen complexes bound to the protein A-coated wells was detected using a GloMax luminometer after injection of 50 μ L/well native coelenterazine substrate. RLUs were read after a two second delay following injection and a five second integration time. Rluc-VP1 antigen treated with pre-immune sera acted as the negative control. The values shown in the table are the highest serum dilutions that gave a RLU count above the negative control + 3 standard deviations. Each serum was diluted to the same intervals (1:40, 1:160, 1:640, 1:2560, 1:10,240, 1:102,400) and tests were performed in duplicate. The duplicate RLU values were averaged and if the average value was above the negative control + 3 standard deviations, the serum dilution was considered positive. The endpoint dilution values were identical in the duplicate wells within each individual assay.

For ELISA titrations, 96-well Nunc-Immuno Maxisorp plates (Thermo Scientific) were coated with VLPs at a concentration of 100 ng/well in PBS and incubated overnight at 4°C. Plates were blocked with 5% nonfat dry milk or BSA in PBS-T for one hour at room temperature and washed with PBS-T. Serum samples were serially diluted in blocking buffer

in a 96-well format as described above. After aliquoting 100 μ L of each serum dilution into wells of the vinyl microtiter plate, 100 μ L of blocking buffer was added to each well. This diluted the sera 1:2 as had occurred in the LIPS assay following the addition of the Rluc-VP1 lysate to the antibody dilutions. A total of 100 μ L of diluted antibody were added in duplicate to VLP-coated plates and incubated at room temperature for one hour. After washing the plates with PBS-T, anti-guinea pig or anti-rabbit HRP-conjugated antibodies (Sigma, diluted 1:1,000 in PBS) were added and incubated for an hour at room temperature. Following four washes with PBS-T, 100 μ L of TMB substrate (Thermo Fisher Scientific) was added to each well and left to incubate at room temperature for 30 minutes before reading the absorbance at 651 nm. The values shown in the table are the highest serum dilutions that gave an O.D. value above the negative control + 3 standard deviations. Each serum was diluted to the same intervals (1:40, 1:160, 1:640, 1:2560, 1:10,240, 1:102,400) and tests were performed in duplicate. The duplicate O.D. values were averaged and if the average value was above the negative control + 3 standard deviations, the serum dilution was considered positive. The endpoint dilution values were identical in the duplicate wells within each individual assay.

2.6.4 HBGA binding assays—Clear and opaque white 96-well Maxisorp plates were coated with either BSA or pig gastric mucin type III (PGM; Sigma) diluted to 100 μ g/mL in PBS and incubated overnight at 4°C. Clear plates were used for VLP binding assays; white plates were used for luciferase-based assays. Plates were then blocked with 5% nonfat dry milk or BSA in PBS-T for one hour at room temperature and washed with PBS-T.

For HBGA binding assays, VLPs or Rluc-VP1 lysates were serially diluted in 5% nonfat dry milk or BSA in PBS-T. Dilutions were added to the BSA- or PGM-coated plates and incubated for an hour at 4°C while rocking. Unbound antigen was removed after four washes with PBS-T. GI.1 NV VLPs bound to the BSA- or PGM-coated wells were detected with a GI.1 NV-specific monoclonal antibody (Abcam). Bound GII.4 MD145 and GII.4 Sydney2012 VLPs were detected using genotype-specific hyperimmune sera diluted 1:2,000 in 5% nonfat dry milk or BSA in PBS-T. After an hour of incubation at room temperature, HRP-conjugated secondary antibodies were diluted 1:5,000 in 5% nonfat dry milk or BSA in PBS-T, added to the wells of the VLP-based approach, and incubated at room temperature for an hour. Wells were washed three times with PBS-T before adding 100 μ L of TMB substrate per well. Absorbances were read at 651 nm after 30 minutes of incubation at room temperature. Following the final PBS-T washes, RlucVP1 bound to BSA- or PGM-coated wells was detected by a GloMax luminometer following machine-injection of 50 μ L native coelenterazine substrate, a two second delay, and a five second integration time.

2.6.5 HBGA blockade assays—Clear and opaque white 96-well Maxisorp plates were coated with pig gastric mucin type III (PGM; Sigma) diluted to 100 μ g/mL in PBS and incubated overnight at 4°C. Clear plates were used for VLP blocking assays; white plates were used for luciferase-based blocking assays. Plates were then blocked with 5% nonfat dry milk or BSA in PBS-T for one hour at room temperature and washed with PBS-T.

For VLP-based blockade assays, VLPs were diluted to 2 μ g/mL in 5% nonfat dry milk or BSA in PBS-T. Serum samples were serially diluted 4-fold in 5% nonfat dry milk or BSA

in PBS-T and added to 96-well vinyl U-bottom plates. A 100 μ L volume of VLPs was added to 100 μ L of each serum dilution, reducing final VLP concentrations to 1 μ g/mL. Following incubation for one hour at 4°C while rocking, 100 μ L of the antibody-VLP mixtures were added in duplicate to PGM-coated wells and incubated for an additional hour at 4°C with rocking. Plates were washed four times with PBS-T. Bound VLPs were measured with detecting antibodies and HRP-conjugated secondary antibodies as described above, taking care that the detecting sera originated from an animal species different from the blocking sera or monoclonal antibody being tested.

For luciferase-based blockade assays, Rluc-VP1 lysates were diluted to 2×10^6 RLU/mL in 5% nonfat dry milk or BSA in PBS-T. Sera and HBGA-blocking monoclonal antibodies were diluted and added to 96-well plates as described above. A 100 μ L volume of Rluc-VP1 lysate was added to 100 μ L of each serum dilution, and the antibody-Rluc-VP1 mixtures were incubated for one hour at 4°C while rocking. Antibody-antigen mixtures were added in duplicate to PGM-coated plates and incubated for an additional hour at 4°C as before. Plates were washed four times with PBS-T, and PGM-bound Rluc-VP1 protein was detected by a GloMax luminometer following machine-injection of 50 μ L native coelenterazine substrate, a two second delay, and a five second integration time.

The 50% blocking titer (BT50) was defined as the serum dilution at which the O.D. or RLU value was 50% of that of the appropriate control. Blockade assays performed with hyperimmune sera were compared to pre-immune serum-treated controls, whereas blockade assays performed with monoclonal antibodies were compared to untreated controls. A BT50 value of <80 was assigned to samples that did not show a 50% decrease in comparison to the control at the lowest serum dilution tested (1:80). Graphs were generated using GraphPad Prism 7.0 and BT50 values were determined using the nonlinear fit – one site logIC50 binding curve analysis (top constraint = 0, bottom constraint = 100).

3. Results

3.1 Expression of Rluc-VP1 fusion proteins in transfected cells

A panel of Rluc-VP1 fusion proteins was constructed by Gateway cloning for use in the luciferase-based HBGA blocking assay, designated here as LIPS-Blockade. Renilla luciferase (Rluc) was fused to the N-terminus of HuNoV major capsid proteins and to the negative control protein, JUN, a component of the transcription factor AP-1 which was not predicted to bind HBGA. Western blot analysis was used to verify the expression of Rluc antigens following transfection into HEK293T cells. Probing with an anti-renilla luciferase monoclonal antibody revealed proteins of 95–110 kDa (Fig. 1A), corresponding to the expected total molecular mass of fusion proteins: ~36 kDa (Rluc) and ~60–75 kDa (HuNoV VP1). Probing the same lysates with hyperimmune guinea pig sera raised against HuNoV VLPs confirmed the fusion of Rluc to HuNoV VP1 (Fig. 1B). Serum raised against the GI.1 NV strain solely reacted with the GI.1 NV Rluc-VP1. Serum raised against the GII.4 MD145 strain recognized both GII.4 Rluc-VP1 fusion proteins from GII.4 MD145 and GII.4 Sydney2012. Anti-MNV serum recognized MNV Rluc-VP1 only.

Two HBGA binding pockets are located at the interface of two VP1 monomers and require dimerization to properly form the pockets and bind HBGAs. Monoclonal antibody D8 has been mapped to the GI.1 NV VP1 dimeric interface and demonstrates efficient HBGA blocking activity (Chen, Sosnovtsev et al. 2013). To determine whether dimeric forms of VP1 were produced in the transfected cell lysates, we tested D8 in the LIPS assay conducted at room temperature (25°C) and 4°C (Fig. 1C). D8 was able to recognize GI.1 NV Rluc-VP1 at both temperatures, with optimal binding at 4°C, consistent with the presence of dimerized Rluc-VP1.

3.2 HBGA binding of HuNoV VLPs and Rluc-VP1 fusion proteins

The utility of Rluc-VP1 antigens in an HBGA blockade assay was investigated by measuring their levels of binding to pig gastric mucin (PGM). PGM contains HBGA-like molecules and has been shown to bind a wide range of HuNoV VLPs (Tian, Brandl et al. 2005). Homologous VLPs were tested for PGM binding alongside the luciferase-tagged VP1 proteins. Both VLPs (Fig. 2A) and Rluc-VP1 lysates (Fig. 2B) were able to bind PGM in a dose-dependent manner and failed to bind BSA at even the highest concentrations tested. While MNV has been shown to bind carbohydrate moieties such as sialic acid, it has failed to bind any synthetic HBGAs (Taube, Perry et al. 2009, Donaldson, Lindesmith et al. 2010). The observed minimal binding of MNV Rluc-VP1 to PGM supported this trend, as any binding to PGM-coated wells was likely due to low amounts of sialic acid being present in the PGM. The VLP control 2117 was derived from a vesivirus, a distant member of the family *Caliciviridae*. The 2117 VLPs and the Rluc control, Rluc-JUN, did not bind BSA or PGM. Taken together with the D8 monoclonal binding observations, these data indicate that the HuNoV Rluc-VP1 proteins are in a dimeric conformation and that the HBGA binding pockets maintain PGM binding capacity. Therefore, the Rluc-VP1 proteins can serve as antigens in the HBGA blockade assay.

3.3 Determination of anti-HuNoV antibody titer in hyperimmune animal sera

The titer of anti-HuNoV antibodies in sera from rabbits and guinea pigs immunized with GI.1 NV and GII.4 MD145 VLPs were determined using both traditional ELISAs and LIPS assays (Table 2). In both assays, sera had the highest recognition when screened with homotypic antigens. The anti-GII.4 MD145 guinea pig serum recognized the antigenically similar GII.4 Sydney2012 VLPs and Rluc-VP1 proteins more efficiently than the anti-GII.4 MD145 rabbit serum. Both anti-GI.1 NV sera showed low reactivity against GII.4 Sydney2012 antigens.

The original LIPS paper reported titers measured by LIPS were either equal or marginally higher than titers measured by ELISA (Tin, Yuan et al. 2017). In our study, most titers measured by LIPS were equal to titers measured by ELISA. The exception to this trend were titers measured against the heterologous antigens, GII.4 Sydney2012 VLPs and Rluc-VP1 proteins. GII.4 Sydney2012 LIPS titers were roughly 4–10-fold higher than ELISA titers. This increased titer may result from increased availability of shared epitopes on the Rluc-VP1 fusion proteins compared to fully formed VLPs. Taken together, these data support previous observations (Tin, Yuan et al. 2017) that the LIPS assay can detect antibodies

that recognize shared and crossreactive epitopes between different genotypes, but less so between different genogroups.

3.4 Detection of HBGA blocking activity in hyperimmune animal sera

To assess whether the Rluc-VP1 proteins could be used to detect HBGA blocking activity, the titers of HBGA blocking antibodies in hyperimmune sera were determined using both the standard HBGA blocking assay and the LIPS-Blockade assay. The amount of PGM-bound antigen that was detected following preincubation with serum was plotted as a percentage relative to pre-immune sera-treated controls. For both the standard VLP-based blocking assay and the luciferase-based approach (Fig. 3A and 3B, respectively), homotypic hyperimmune sera demonstrated the most efficient blocking activity. Rabbit anti-GI.1 NV serum blocked GI.1 NV antigen binding in both assays, whereas the guinea pig anti-GI.1 NV serum failed to block at least 50% of antigen binding in either assay. Both guinea pig and rabbit sera raised against GII.4 MD145 blocked MD145 VLP and Rluc-VP1 binding to PGM. However, only guinea pig anti-GII.4 MD145 serum demonstrated blocking activity when tested against the closely related GII.4 Sydney2012 antigens. In all cases, the blocking activity observed in the standard VLP-based blocking assay was also detected in the luciferase-based assay.

BT50 values were calculated using nonlinear fit IC₅₀ curves (Fig. 3C). The luciferase-based HBGA blockade assay determined BT50 values for polyclonal sera that were roughly 2fold higher than the standard assay. Contrary to this trend, almost identical BT50s of GII.4 Sydney2012-specific monoclonal antibodies G2 and G5 were obtained in both assays. GII.4–2012-G2, which blocks GII.4 Sydney2012 at an uncharacterized blockade epitope (Lindesmith, Brewer-Jensen et al. 2017), achieved a BT50 of 80 ng/mL in the LIPS-Blockade assay, compared to 90 ng/mL in the VLP-based blockade assay. Similarly, GII.4–2012-G5, which blocks the well-characterized Epitope A unique to GII.4 Sydney2012, achieved a BT50 of 64 ng/mL and 75 ng/mL using GII.4 Sydney2012 VLPs and Rluc-VP1, respectively. These data demonstrated that both HBGA blocking assays can be used to determine blocking antibody titers for hyperimmune sera as well as monoclonal antibodies.

3.5 Comparison of HBGA blockade antibody profiles detected by Rluc-VP1 proteins and by VLPs

To determine whether antibodies measured in the luciferase-based HBGA blocking assay were similar to those quantified in the standard VLP-based assay, a competitive HBGA blocking assay was performed. As outlined in Figure 4A, sera or antibodies of interest were incubated with either homotypic or heterotypic VLPs (1.). Antibody-VLP mixtures were then added to clear PGM-coated plates to adsorb unblocked VLPs to the PGM (2.); VLPs whose HBGA binding remained intact following antibody treatment would preferentially bind PGM rather than remain in solution and potentially compete with Rluc-VP1 for binding in the final ligand binding step. The unbound antibodies were subsequently added to Rluc-VP1 lysate (3.), incubated for an hour at 4°C, and added to fresh white plates coated with PGM (4.). Plates were washed (5.) and changes in HBGA blockade titer were measured (6.). Positive competition was defined as VLP pretreatment that significantly reduced blockade titers against Rluc-VP1 compared to the “No VLP” control.

VLP competition was only detectable when homotypic VLPs and Rluc-VP1 antigens were used to assess competitive blocking activity. When anti-GII.4 MD145 guinea pig serum was incubated with the panel of VLPs, only GII.4 MD145 VLPs removed a significant population of blocking antibodies reactive against GII.4 MD145 Rluc-VP1 (Fig. 4B). Preincubation with homologous GII.4 MD145 VLPs resulted in a 6.5-fold reduction in the BT50 titer (i.e., a lower dilution of serum), therefore higher levels of serum antibody were required to block 50% of the binding. Preincubation with GI.1 NV and GII.4 Sydney2012 VLPs had no effect on the BT50 compared to the untreated control, which also provided evidence that nonblocked VLPs were effectively removed from the solution in Step 2 and did not compete with Rluc-VP1 for the final PGM binding step. Preincubation of the GII.4 Sydney2012 monoclonal antibody, GII.4–2012-G5, with the panel of VLPs yielded similar competitive blocking patterns (Fig. 4C). Preincubation with homologous GII.4 Sydney2012 VLPs yielded a BT50 value 6.8-fold higher than the untreated control (i.e., more monoclonal antibody was required to block 50% of GII.4 Sydney2012 Rluc-VP1 binding), while preincubation with GI.1 NV and GII.4 MD145 VLPs did not significantly increase the BT50 value (Fig. 4D). These data demonstrate that both the VLP-based and luciferase-based HBGA blocking assays measure the same blockade antibody activity.

3.6 HBGA blockade antibody responses following viral challenge and natural HuNoV infection

To monitor blockade antibody titer changes after HuNoV infection, HuNoV-specific titers (Fig. 5A) and HBGA blockade titers (Fig. 5B) of chimpanzee and human sera collected pre- and post-infection were characterized using VLPs and Rluc-VP1 antigens. As part of an animal model study, chimpanzees were orally challenged with live GI.1 NV (Bok, Parra et al. 2011). One sampled chimpanzee gained broadly reactive anti-HuNoV antibodies at a titer of 1.0×10^4 after challenge, with GI.1-specific antibody titers detected at a \log_{10} higher serum dilution. HBGA blockade was only detected against GI.1 NV VLPs and Rluc-VP1 proteins, demonstrating the genogroup specificity of the LIPS-Blockade assay.

Four adult volunteers were previously challenged with Cin-1, a GII.4 strain most closely related to outbreak strain Farmington Hills 2002 (accession number JQ965810) (Frenck, Bernstein et al. 2012). Sera was collected at Day 0 and Day 30 post-challenge. Post-challenge sera from these patients (Pt) contained 1–2 \log_{10} higher antibody titers against each VLP or Rluc-construct, except Pt5 who had modest increases (4–10-fold) in titer against GI.1 NV and GII.4 MD145 (Fig. 5A). Each pre-challenge serum contained no detectable levels of HBGA blockade against VLPs (Fig. 5B). Pre-challenge sera screened with GII.4 MD145 Rluc-VP1 proteins demonstrated low levels of HBGA blockade, possibly reflecting low levels of immunity from previous GII.4 exposures that the VLP-based assay could not detect (Fig. 5B). Post-challenge sera from all patients contained 1–2.2 \log_{10} higher BT50s against GII.4 MD145 VLPs and Rluc-VP1 proteins. Patients 3 and 5 interestingly gained some limited cross-blockade activity against the later circulating GII.4 strain, Sydney2012. No sera demonstrated HBGA blockade against GI.1 NV VLPs or Rluc-VP1 proteins.

Finally, serum samples from a naturally infected patient under treatment at Erasmus Medical Center (EMC003) were collected prior to infection (Day -3) and several weeks following infection (Day 46). Sequencing analysis revealed they were infected with the HuNoV strain GII.4 New Orleans 2009 [GII.P4] (accession number MT929247) (van Beek, de Graaf et al. 2016). Three days prior to HuNoV exposure, the patient's anti-HuNoV recognizing titers were low ($<10^3$) against all strains (Fig. 5A). At 46 days post-infection, a 1–2 \log_{10} boost in antibody titer was observed against all antigens, with the largest increase observed for antibodies that recognized related GII.4 strains. The anti-GII.4 MD145 antibodies present in the patient's pre-infection serum demonstrated some HBGA blockade activity against both Rluc-VP1 and VLPs, though the blocking antibodies were low in titer (Fig. 5B). No other blockade patterns were observed for the sera collected at Day -3. Following the boost in humoral immunity post-infection at Day 46, the HBGA BT50 against GII.4 MD145 increased 7-fold. Additionally, the infection with a GII.4 New Orleans 2009 strain gave rise to antibodies that could block the later-circulating GII.4 Sydney2012 strains, both VLPs and Rluc-VP1 proteins. Neither serum was able to block GI.1 NV VLPs or Rluc-VP1 proteins.

Taken together, these data indicate that the Rluc-VP1 system can detect and profile the specificity of a serologic response following natural infection, and that the newly developed LIPS-Blockade assay can serve to characterize the HBGA blocking activity of these antibodies.

4. Discussion

A LIPS-Blockade assay was established for the detection of potentially protective anti-HuNoV antibodies in polyclonal sera. Our aim was to develop an assay that was readily scalable, allowed for the rapid generation of novel antigens, and not dependent on the availability of VLPs. In addition, the assay would need to perform comparably to the gold standard VLP-based HBGA blocking assay.

First, we demonstrated that the renilla-tagged capsid protein could bind HBGA-containing PGM. The assessment with the monoclonal antibody D8 provided evidence that the Rluc-VP1 fusion proteins maintained the capacity to dimerize and did so more efficiently at lower temperatures (Fig. 1C). We also observed that Rluc-VP1 proteins bound PGM better at 4°C, consistent with the idea that Rluc-VP1 dimerization is temperature sensitive (data not shown). We suspect that the decreased temperature stabilized the structural integrity of the HBGA binding sites and may have also compensated for any steric hindrance caused by the N-terminal addition of Rluc, thereby allowing dimerization to occur more readily. This choice of temperature for assay performance, however, comes with the caveat that lower temperatures favor antibodies binding at more surface-exposed epitopes and decreased access to more buried epitopes within the VLP structure (Lindsmith, Mallory et al. 2018). Biologically relevant access to these hidden epitopes may therefore be better studied using VLP-based methods.

Immunization and infection in both animals and humans led to stimulation of cross-genogroup anamnestic responses as measured by LIPS and ELISA, though homotypic recognizing titers were expectedly higher than cross-genotype titers. Anamnestic antibody

responses have been linked to the presence of shared epitopes among norovirus strains, as has been reported in previous outbreak and challenge studies [reviewed in (van Loben Sels and Green 2019).] Variations in blocking activity demonstrated that the LIPS-Blockade assay could readily distinguish between bulk antibody binding to antigen and its HBGA blocking activity. The blocking activity of the anti-GII.4 MD145 guinea pig serum against the GII.4 Sydney2012 RlucVP1 fusion protein demonstrated that the assay is also able to detect cross-reactivity with antigenically related strains. This limited, cross-reactive blocking was only observed when sera were screened with antigens of the same genotype (e.g., treating GII.4 sera against related GII.4 VLPs and Rluc-VP1 proteins). HBGA binding of the GI.1 NV Rluc-VP1 protein was not blocked with GI.3 sera; similarly, pretreatment of GII.4 MD145 and GII.4 Sydney2012 Rluc-VP1 proteins with GII.2 or GII.3 sera also had no effect on HBGA binding (data not shown). The VLP competition assay provided further evidence that the assays maintained comparable specificity when detecting HBGA blockade antibodies. Only homotypic VLPs competed for blockade antibodies, thus demonstrating that both assays were able to quantify the same blocking antibody population.

Because the animal sera used in Figure 3 was generated via IM injection and was highly strain specific, we wanted to confirm that the LIPS-Blockade assay is capable of measuring HBGA blockade in complex sera following natural infection or oral challenge. A panel of human and primate sera was characterized for HuNoV-specific reactivity and HBGA blockade activity using the LIPS and LIPS-Blockade assays, respectively. Each HuNoV exposure resulted in an increase in genotype-restricted HBGA blocking antibodies that could be detected in the LIPSBlockade assay. The chimpanzee challenged with GI.1 NV developed GI.1-specific HBGA blockade antibodies post-challenge. Four individuals challenged with a 2002 GII.4 strain (Cin-1) developed blockade antibodies that recognized an earlier circulating GII.4 strain from 1987 (MD145), with two of these responses also recognizing a future GII.4 strain from 2012 (Sydney2012). Finally, the pre-infection serum of a patient naturally infected with a 2009 GII.4 strain showed the presence of pre-existing blockade antibodies against GII.4 MD145 that were boosted in their post-infection sera. After HuNoV infection, a new HBGA blockade antibody population was also detected in this patient that blocked GII.4 Sydney2012. Thus, changes in titer and the generation of new HBGA blockade activity can both be detected with the LIPS-Blockade assay. Each increase in recognizing titer and generation of HBGA blockade antibodies were detected by both VLP- and Rluc-VP1-based assays, confirming that strain-specific, serological responses in patients can be characterized using the Rluc-VP1 platforms.

It was previously reported that binding titers in sera were higher when screened with the HuNoV LIPS assay as compared to a standard ELISA assay (Tin, Yuan et al. 2017). We observed a similar trend with the luciferase based HBGA blockade assay. Polyclonal human and animal sera had BT50 values roughly twice as high when measured with Rluc-VP1 as opposed to VLPs. However, the differences between BT50 values achieved by both assays was not statistically significant when using monoclonal antibodies (Fig. 3C). The increased BT50s in polyclonal sera were possibly observed due to increased exposure of common epitopes on luciferase-tagged proteins compared to their VLP counterparts. Likely located in the shell domain, these epitopes would usually be buried inside of VLPs and therefore would be less accessible to antibody recognition in VLP-based assays (Hansman, Taylor et

al. 2012, Parra, Abente et al. 2012, Parra, Azure et al. 2013). Antibodies that recognize these buried epitopes on dimeric Rluc-VP1 may possess direct HBGA blocking activity, they may sterically hinder HBGA binding, or they may work allosterically to induce conformational changes in nearby HBGA binding epitopes. Thus, less antibody would be required for the LIPS-Blockade assay to achieve the same BT50 of the VLP-based assay due to increased epitope availability.

As highlighted with the previously developed HuNoV LIPS assay, the limitations of our current study included the possibility of conformational epitopes misfolding due to the N-terminal addition of Rluc. However, immunofluorescence staining and blockade of GI.1 NV and GII.4 Sydney2012 Rluc-VP1 with the strain-specific monoclonal antibodies provided evidence that some well-established immunodominant epitopes such as GII.4 Epitope A remained intact (data not shown, Fig. 3C). Future studies are needed to assess the presentation of other important blockade and non-blockade epitopes encoded elsewhere on Rluc-VP1. The addition of VP2, a minor structural protein, may also influence structure and immunogenicity of Rluc-VP1 constructs and would be of interest to study in the future.

There are several advantages of the LIPS-Blockade assay. Sequencing patient-specific strains of HuNoV and creating matching Rluc-VP1 antigens can in many instances be more rapid than generating matching VLPs. By not relying on VP1 to self-assemble into full VLPs, the LIPS-Blockade assay provides a quick, personalized, and scalable platform for screening immunologically important antibodies. Additionally, mutagenesis studies to map functional domains may be simpler with Rluc-VP1 proteins than with VLPs, as certain mutations in the VP1 protein may prevent proper VLP assembly. Finally, the time, technical demand, infrastructure requirement, and costs associated with producing Rluc-VP1 proteins are lower than those of HuNoV VLPs. Therefore, the LIPS-Blockade assay may be more feasible for laboratories with restricted time and budgetary resources or for laboratories where access to the required equipment (e.g. ultracentrifuge) is not possible. We would highlight that, while this assay is useful for certain applications such as large-scale screening, it may not be a suitable replacement for others, such as detailed study of conformational blockade epitopes presented by an intact virion.

In conclusion, this study provides evidence that HuNoV Rluc-VP1 fusion proteins can be used to rapidly assess both anti-HuNoV antibody titers as well as potentially protective HBGA blockade titers. Widespread implementation of this system therefore has the potential to provide invaluable insights into the immune responses to HuNoVs in naturally infected populations.

Supplementary Material

Refer to Web version on PubMed Central for supplementary material.

Acknowledgments

We thank Dr. Alexis de Rougemont for the baculovirus stocks and Pr. Jürgen Haas for the Gateway pDONR vector. We thank Dr. Xi (Jason) Jiang of the Cincinnati Children's Hospital Medical Center, Cincinnati, Ohio, for providing paired human sera for this study.

Funding

Funding for this work was provided by the Wellcome Trust [207498/Z/17/Z] (IGG); the Division of Intramural Research of the National Institute of Allergy and Infectious Diseases, NIH (KYG); COMPARE grant agreement N°643476 (MPGK) and MRACE grant 2017 (MdG); and National Institute of Allergy and Infectious Diseases, NIH grants R01 AI148260, R56 AI106006, U19 AI109761 CETR, and the Wellcome Trust [203268/Z/16/Z] (RSB).

References

- Atmar RL, Bernstein DI, Harro CD, Al-Ibrahim MS, Chen WH, Ferreira J, Estes MK, Graham DY, Opekun AR, Richardson C and Mendelman PM. (2011). “Norovirus vaccine against experimental human Norwalk Virus illness.” *N Engl J Med* 365(23): 2178–2187. [PubMed: 22150036]
- Atmar RL, Ettayebi K, Ayyar BV, Neill FH, Braun RP, Ramani S and Estes MK. (2019). “Comparison of Microneutralization and Histo-blood Group Antigen-Blocking Assays for Functional Norovirus Antibody Detection.” *J Infect Dis*.
- Bartsch SM, Lopman BA, Hall AJ, Parashar UD and Lee BY. (2012). “The potential economic value of a human norovirus vaccine for the United States.” *Vaccine* 30(49): 7097–7104. [PubMed: 23026689]
- Bartsch SM, Lopman BA, Ozawa S, Hall AJ and Lee BY. (2016). “Global Economic Burden of Norovirus Gastroenteritis.” *PLoS One* 11(4): e0151219.
- Bok K, Parra GI, Mitra T, Abente E, Shaver CK, Boon D, Engle R, Yu C, Kapikian AZ, Sosnovtsev SV, Purcell RH and Green KY. (2011). “Chimpanzees as an animal model for human norovirus infection and vaccine development.” *Proc Natl Acad Sci U S A* 108(1): 325–330. [PubMed: 21173246]
- Chen Z, Sosnovtsev SV, Bok K, Parra GI, Makiya M, Agulto L, Green KY and Purcell RH. (2013). “Development of Norwalk virus-specific monoclonal antibodies with therapeutic potential for the treatment of Norwalk virus gastroenteritis.” *J Virol* 87(17): 9547–9557. [PubMed: 23785216]
- Chhabra P, de Graaf M, Parra GI, Chan MC, Green K, Martella V, Wang Q, White PA, Katayama K, Vennema H, Koopmans MPG and Vinje J. (2019). “Updated classification of norovirus genogroups and genotypes.” *J Gen Virol*.
- Donaldson EF, Lindesmith LC, Lobue AD and Baric RS. (2010). “Viral shape-shifting: norovirus evasion of the human immune system.” *Nat Rev Microbiol* 8(3): 231–241. [PubMed: 20125087]
- Ettayebi K, Crawford SE, Murakami K, Broughman JR, Karandikar U, Tenge VR, Neill FH, Blutt SE, Zeng X-L, Qu L, Kou B, Opekun AR, Burrin D, Graham DY, Ramani S, Atmar RL and Estes MK. (2016). “Replication of human noroviruses in stem cell-derived human enteroids.”
- Frenck R, Bernstein DI, Xia M, Huang P, Zhong W, Parker S, Dickey M, McNeal M and Jiang X. (2012). “Predicting susceptibility to norovirus GII.4 by use of a challenge model involving humans.” *J Infect Dis* 206(9): 1386–1393. [PubMed: 22927452]
- Glass PJ, Zeng CQ and Estes MK. (2003). “Two nonoverlapping domains on the Norwalk virus open reading frame 3 (ORF3) protein are involved in the formation of the phosphorylated 35K protein and in ORF3-capsid protein interactions.” *J Virol* 77(6): 3569–3577. [PubMed: 12610132]
- Hansman GS, Taylor DW, McLellan JS, Smith TJ, Georgiev I, Tame JR, Park SY, Yamazaki M, Gondaira F, Miki M, Katayama K, Murata K and Kwong PD. (2012). “Structural basis for broad detection of genogroup II noroviruses by a monoclonal antibody that binds to a site occluded in the viral particle.” *J Virol* 86(7): 3635–3646. [PubMed: 22278249]
- Hardy ME. (2005). “Norovirus protein structure and function.”
- Hoffmann S, Batz MB and Morris JG Jr. (2012). “Annual cost of illness and quality-adjusted life year losses in the United States due to 14 foodborne pathogens.” *J Food Prot* 75(7): 1292–1302. [PubMed: 22980013]
- Hopkins R and Esposito D. (2009). “A rapid method for titrating baculovirus stocks using the Sf-9 Easy Titer cell line.” *Biotechniques* 47(3): 785–788. [PubMed: 19852765]
- Iturriza-Gomara M and O’Brien SJ. (2016). “Foodborne viral infections.” *Curr Opin Infect Dis*.
- Jiang X, Wang M, Wang K and Estes MK. (1993). “Sequence and genomic organization of Norwalk virus.” *Virology* 195(1): 51–61. [PubMed: 8391187]

- Jones MK, Grau KR, Costantini V, Kolawole AO, de Graaf M, Freiden P, Graves CL, Koopmans M, Wallet SM, Tibbetts SA, Schultz-Cherry S, Wobus CE, Vinje J and Karst SM. (2015). "Human norovirus culture in B cells." *Nat Protoc* 10(12): 1939–1947. [PubMed: 26513671]
- Lindsmith L, Moe C, Marionneau S, Ruvoen N, Jiang X, Lindblad L, Stewart P, LePendu J and Baric R. (2003). "Human susceptibility and resistance to Norwalk virus infection." *Nat Med* 9(5): 548–553. [PubMed: 12692541]
- Lindsmith LC, Brewer-Jensen PD, Mallory ML, Debbink K, Swann EW, Vinje J and Baric RS. (2017). "Antigenic characterization of a novel recombinant GII.P16-GII.4 Sydney norovirus strain with minor sequence variation leading to antibody escape." *J Infect Dis*.
- Lindsmith LC, Donaldson EF and Baric RS. (2011). "Norovirus GII.4 strain antigenic variation." *J Virol* 85(1): 231–242. [PubMed: 20980508]
- Lindsmith LC, Ferris MT, Mullan CW, Ferreira J, Debbink K, Swanstrom J, Richardson C, Goodwin RR, Baehner F, Mendelman PM, Bargatze RF and Baric RS. (2015). "Broad blockade antibody responses in human volunteers after immunization with a multivalent norovirus VLP candidate vaccine: immunological analyses from a phase I clinical trial." *PLoS Med* 12(3): e1001807.
- Lindsmith LC, Mallory ML, Debbink K, Donaldson EF, Brewer-Jensen PD, Swann EW, Sheahan TP, Graham RL, Beltramello M, Corti D, Lanzavecchia A and Baric RS. (2018). "Conformational Occlusion of Blockade Antibody Epitopes, a Novel Mechanism of GII.4 Human Norovirus Immune Evasion." *mSphere* 3(1).
- Lindsmith LC, McDaniel JR, Changela A, Verardi R, Kerr SA, Costantini V, Brewer-Jensen PD, Mallory ML, Voss WN, Boutz DR, Blazeck JJ, Ippolito GC, Vinje J, Kwong PD, Georgiou G and Baric RS. (2019). Sera Antibody Repertoire Analyses Reveal Mechanisms of Broad and Pandemic Strain Neutralizing Responses after Human Norovirus Vaccination. *Immunity*. 50: 1530–1541 e1538. [PubMed: 31216462]
- Parra GI, Abente EJ, Sandoval-Jaime C, Sosnovtsev SV, Bok K and Green KY. (2012). "Multiple antigenic sites are involved in blocking the interaction of GII.4 norovirus capsid with ABH histo-blood group antigens." *J Virol* 86(13): 7414–7426. [PubMed: 22532688]
- Parra GI, Azure J, Fischer R, Bok K, Sandoval-Jaime C, Sosnovtsev SV, Sander P and Green KY. (2013). "Identification of a Broadly Cross-Reactive Epitope in the Inner Shell of the Norovirus Capsid." *PLoS One* 8(6): e67592.
- Patel MM, Widdowson MA, Glass RI, Akazawa K, Vinje J and Parashar UD. (2008). "Systematic literature review of role of noroviruses in sporadic gastroenteritis." *Emerg Infect Dis* 14(8): 1224–1231. [PubMed: 18680645]
- Ramani S, Neill FH, Ferreira J, Treanor JJ, Frey SE, Topham DJ, Goodwin RR, Borkowski A, Baehner F, Mendelman PM, Estes MK and Atmar RL. (2017). "B-Cell Responses to Intramuscular Administration of a Bivalent Virus-Like Particle Human Norovirus Vaccine." *Clin Vaccine Immunol* 24(5).
- Reeck A, Kavanagh O, Estes MK, Opekun AR, Gilger MA, Graham DY and Atmar RL. (2010). "Serological correlate of protection against norovirus-induced gastroenteritis." *J Infect Dis* 202(8): 1212–1218. [PubMed: 20815703]
- Taube S, Perry JW, Yetming K, Patel SP, Auble H, Shu L, Nawar HF, Lee CH, Connell TD, Shayman JA and Wobus CE. (2009). "Ganglioside-linked terminal sialic acid moieties on murine macrophages function as attachment receptors for murine noroviruses." *J Virol* 83(9): 4092–4101. [PubMed: 19244326]
- Tian P, Brandl M and Mandrell R. (2005). "Porcine gastric mucin binds to recombinant norovirus particles and competitively inhibits their binding to histo-blood group antigens and Caco-2 cells." *Lett Appl Microbiol* 41(4): 315–320. [PubMed: 16162137]
- Tin CM, Yuan L, Dexter RJ, Parra GI, Bui T, Green KY and Sosnovtsev SV. (2017). "A Luciferase Immunoprecipitation System (LIPS) assay for profiling human norovirus antibodies." *J Virol Methods* 248: 116–129. [PubMed: 28673856]
- van Beek J, de Graaf M, Xia M, Jiang X, Vinje J, Beersma M, de Bruin E, van de Vijver D, Holwerda M, van Houten M, Buisman AM, van Binnendijk R, Osterhaus A, van der Klis F, Vennema H and Koopmans MPG. (2016). "Comparison of norovirus genogroup I, II and IV seroprevalence among children in the Netherlands, 1963, 1983 and 2006." *J Gen Virol* 97(9): 2255–2264.

- Van Dycke J, Ny A, Conceição-Neto N, Maes J, Hosmillo M, Cuvry A, Goodfellow I, Nogueira TC, Verbeken E, Matthijssens J, de Witte P, Neyts J and Rocha-Pereira J. (2019). "A robust human norovirus replication model in zebrafish larvae." *PLoS Pathog* 15(9): e1008009.
- van Loben Sels J and Green K. (2019). "The Antigenic Topology of Norovirus as Defined by B and T Cell Epitope Mapping: Implications for Universal Vaccines and Therapeutics." *Viruses* 11(5).

Author Manuscript

Author Manuscript

Author Manuscript

Author Manuscript

Highlights

- Human norovirus capsid protein was tagged with luciferase and recognized HBGAs
- Norovirus-specific blockade assays were developed with the tagged capsid proteins
- Luciferase-based blockade assays circumvent the need for VLPs in antibody profiling

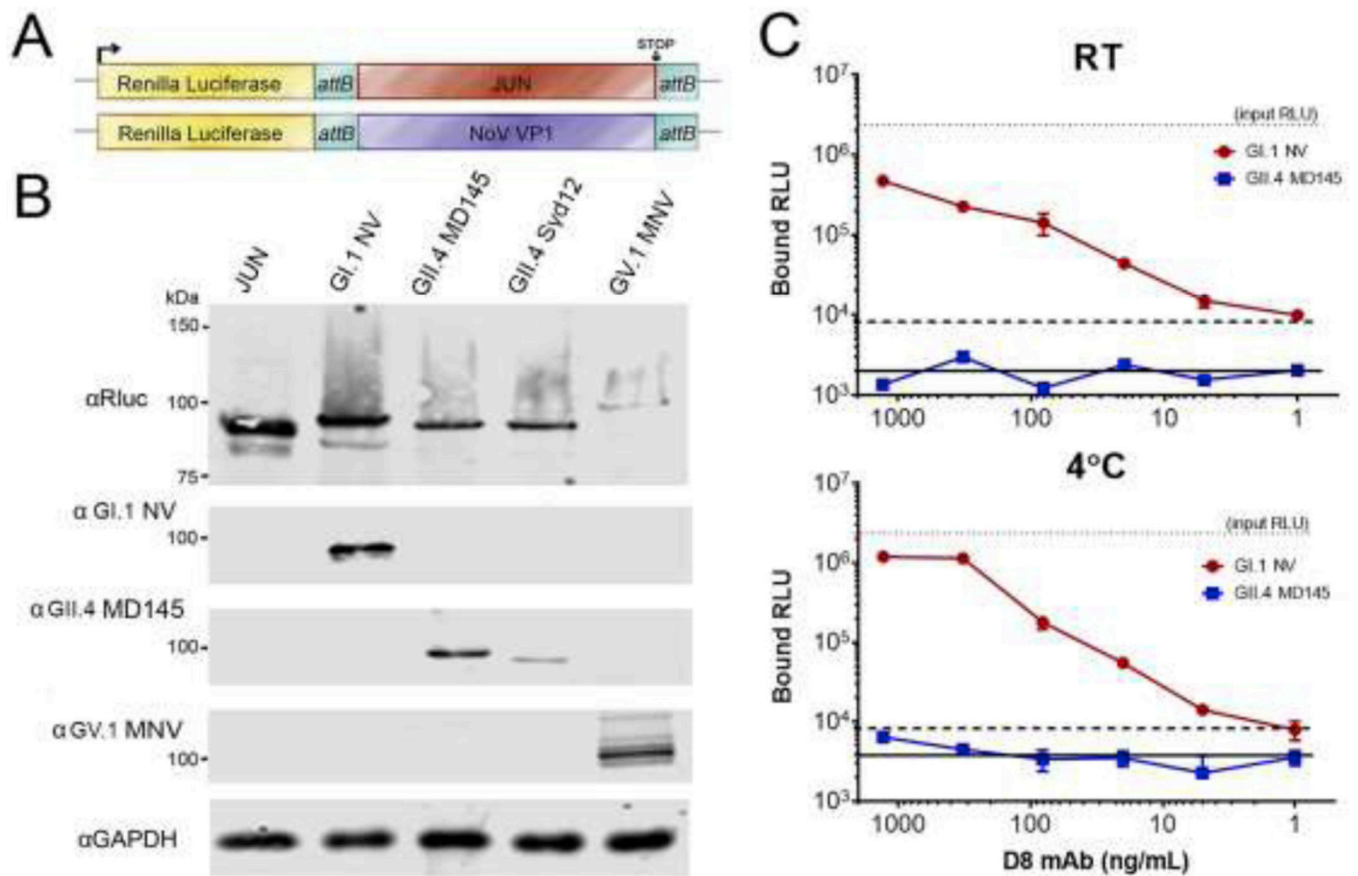


Fig 1. Expression of Rluc fusion proteins.

A) Gateway cloning was used to fuse renilla luciferase (Rluc) to the N-terminus of HuNoV VP1 or the negative control protein, JUN. B) Western blots of HEK293T lysates transfected with Rluc-JUN and HuNoV Rluc-VP1 constructs were probed with an anti-Rluc monoclonal antibody and hyperimmune guinea pig sera raised against GI.1 NV, GII.4 MD145, and GV.1 MNV VLPs. GAPDH acted as the loading control. C) A LIPS assay was performed using the D8 monoclonal antibody which recognized a conformational epitope that spans the dimer interface of two GI.1 NV VP1 proteins. The assay was performed with GI.1 NV and GII.4 MD145 Rluc-VP1 at 4°C and room temperature (25°C). The dotted line represents RLU readings for input Rluc-VP1. Cutoff values were calculated based off of the average of the negative control readings (D8 treated-JUN Rluc-VP1, bold line) plus three standard deviations (dashed line).

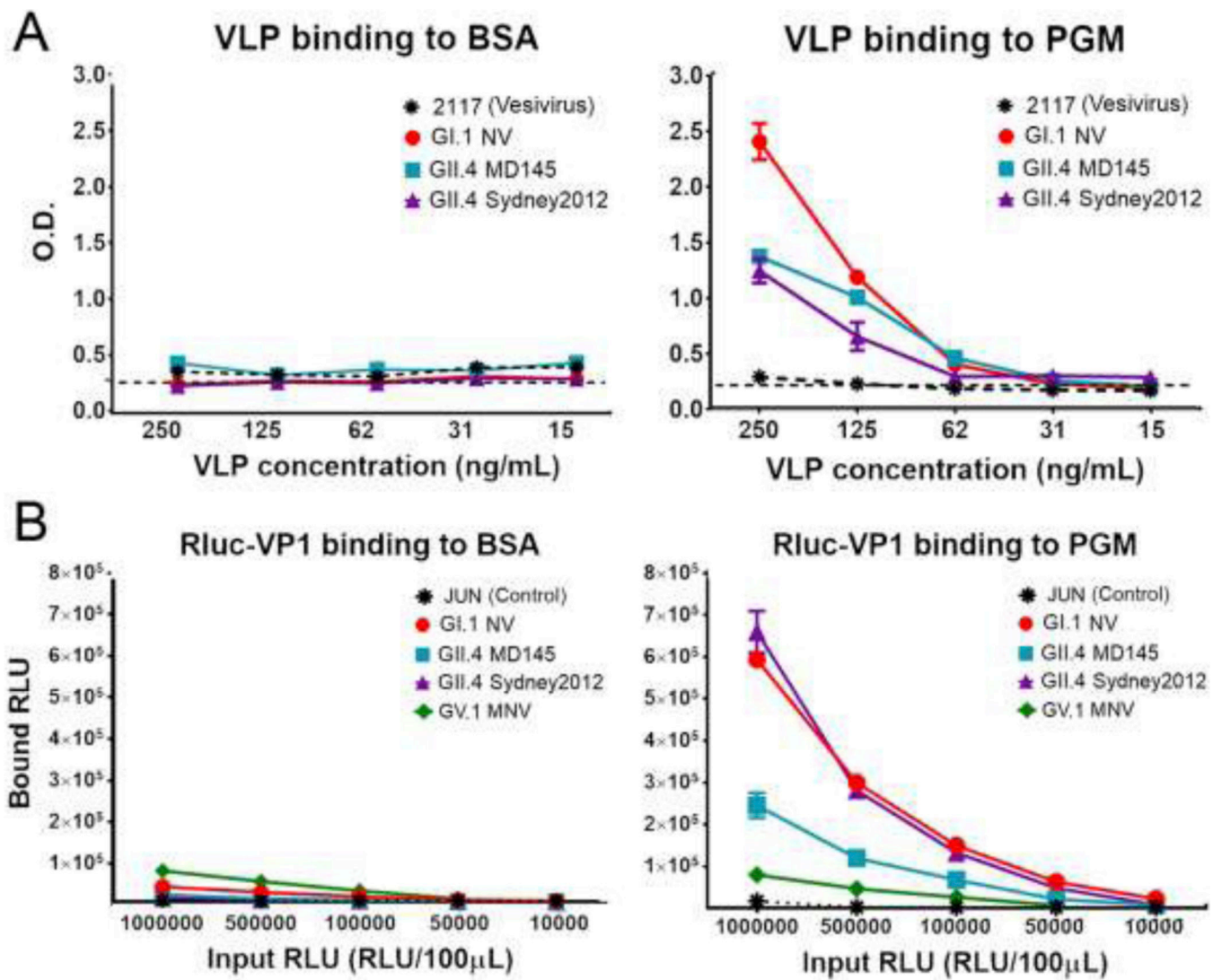


Fig 2. Norovirus VLPs and Rluc-VP1 fusion proteins bound PGM specifically.

A) Clear maxisorp plates coated with 100 μ g/mL of either BSA or PGM were treated with serially diluted concentrations of HuNoV and 2117 (Vesivirus) VLPs. PGM-bound VLPs were detected by corresponding hyperimmune sera. Measurements are represented as average O.D., and error bars represent standard error of the mean. The dashed line represents average O.D. for background signal. B) Plates coated with 100 μ g/mL of PGM or BSA were treated with serially diluted concentrations HuNoV Rluc-VP1 and Rluc-JUN. PGM-bound Rluc proteins were detected by reading luciferase activity of wells following several washes on a GloMax luminometer. Measurements are represented as average bound RLU versus average input RLU/100 μ L. Assays were performed at 4°C.

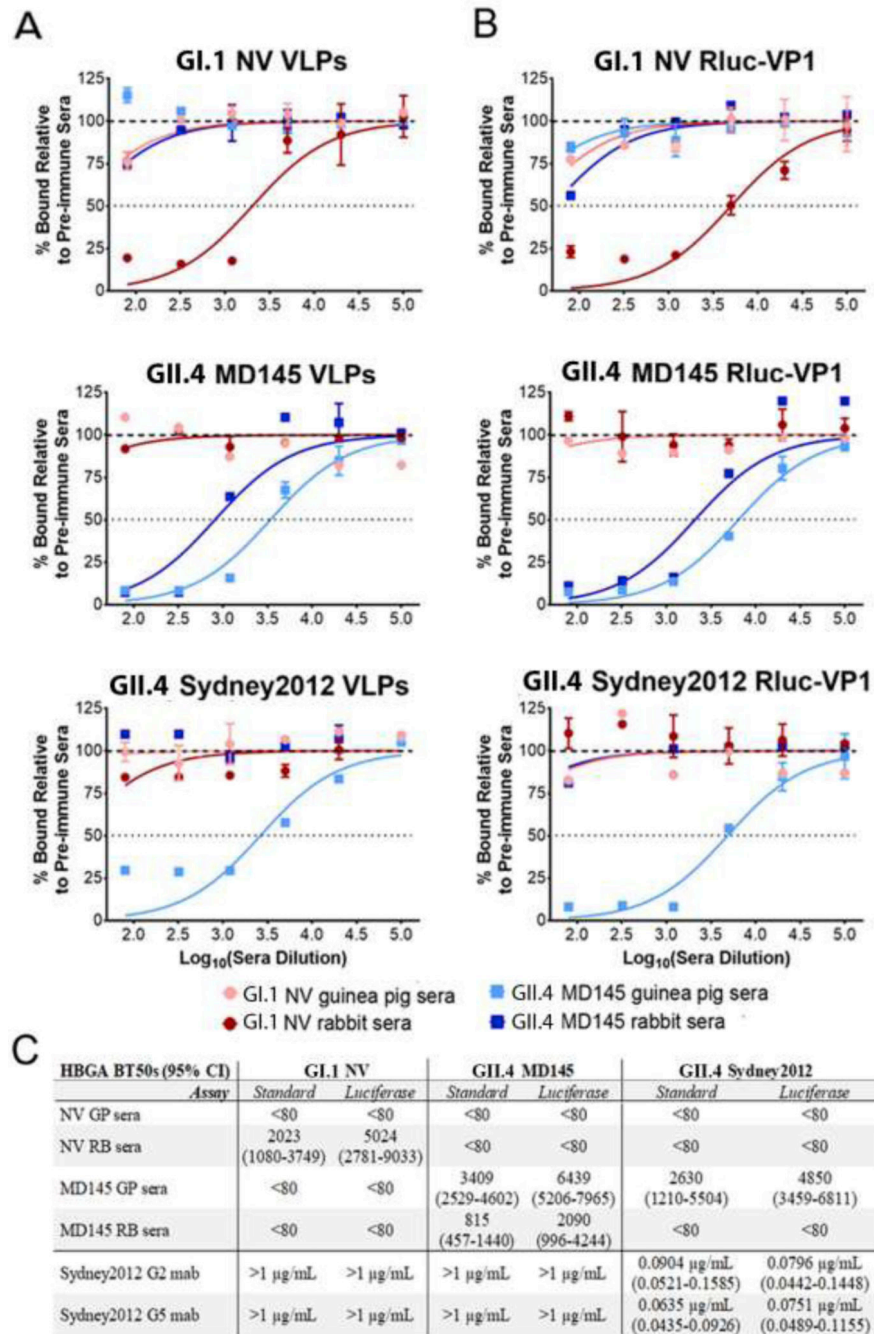


Fig 3. Hyperimmune animal sera blocked antigen binding to PGM.

HuNoV VLPs (A) and Rluc-VP1 proteins (B) were preincubated with serially diluted pre-immune and hyperimmune anti-HuNoV animal sera before being added to plates coated with PGM. Unbound antigen was washed from the plates, and bound antigen was detected either via HRP (VLPs) or luciferase activity (Rluc-VP1 proteins). Graphs report O.D. and RLU values relative to pre-immune controls, with error bars representing SEM. C) HBGA BT50 values were calculated using nonlinear fit – one site logIC₅₀ curve equations with top and bottom constraints 0 and 100, respectively. Values for polyclonal sera were

determined relative to pre-immune-treated controls to account for nonspecific blocking. Values for monoclonal antibodies were determined relative to untreated controls. Values for 95% confidence intervals are reported in parentheses. Sera and monoclonal antibodies that failed to achieve measurable BT50 values are denoted with <80 and >1ug/mL, respectively

Author Manuscript

Author Manuscript

Author Manuscript

Author Manuscript

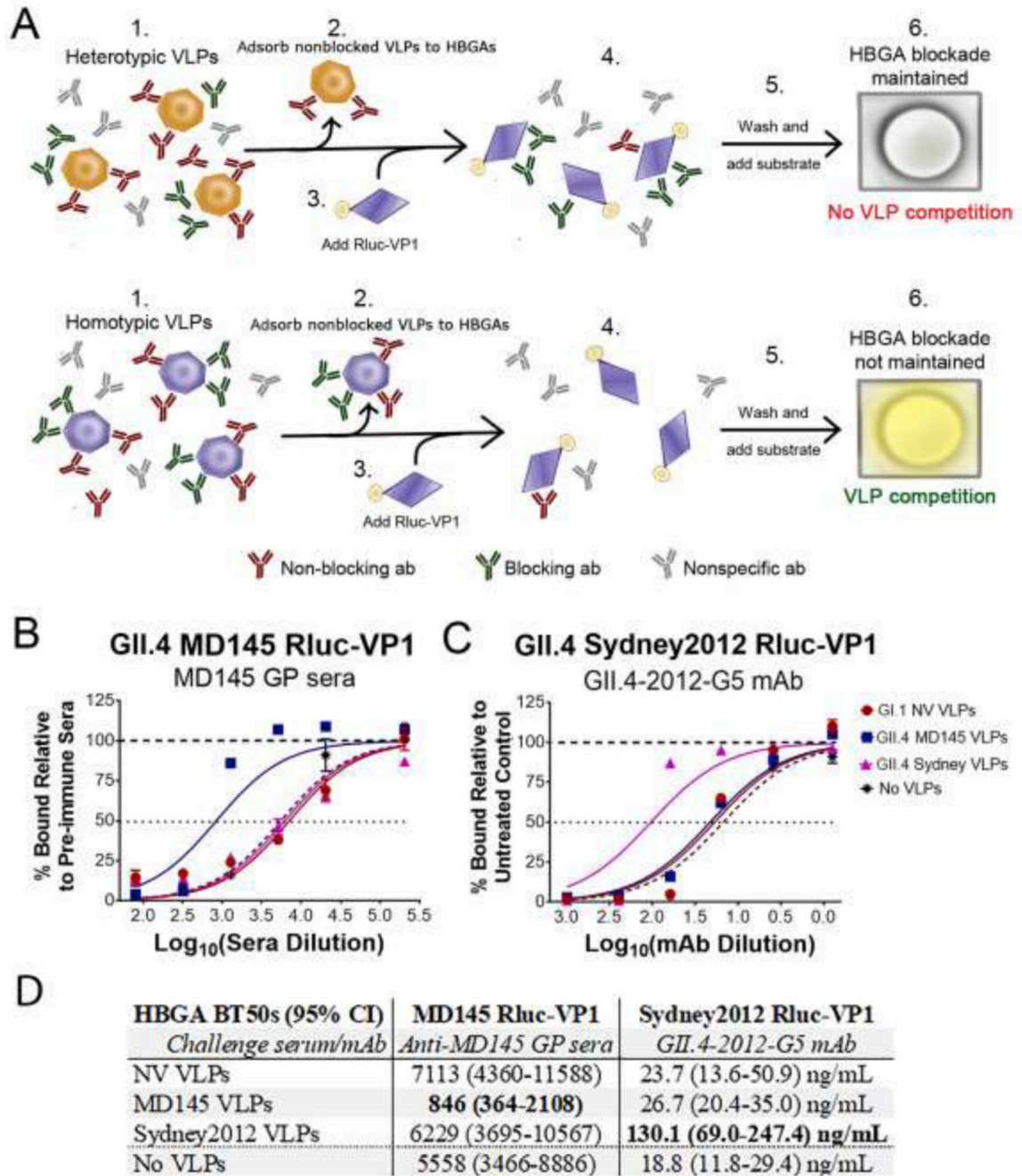


Fig 4. VLPs compete with homotypic Rluc-VP1 for blockade antibodies.

A) Illustration of competitive HBGA blockade assay. 1. Homotypic or heterotypic VLPs were preincubated with serially diluted sera in vinyl 96-well plates for an hour. 2. VLP-antibody mixtures were added to clear maxisorp plates coated with PGM and incubated for an hour. The HBGAs bound (trapped) non-blocked VLPs, theoretically leaving the remaining unbound antibody in the solution. 3. The “unbound” solution was pipetted from the clear maxisorp plates, mixed with Rluc-VP1 proteins in vinyl 96-well plates, and incubated for an hour at 4°C. 4. Rluc-VP1-antibody mixtures were added to fresh

white plates coated with PGM and incubated for an hour at 4°C. 5. White plates were washed with PBS-T, and substrate was added. 6. Luminescence was read by luminometer. If RLuc-VP1 blocking was reduced following VLP pretreatment, marked by an increase in RLU detected in PGM-coated wells, then VLP competition had taken place. B,C) RLuc-VP1 binding percentages were graphed and determined relative to pre-immune sera-treated controls (GII.4 MD145 guinea pig serum) or untreated controls (GII.4 Sydney2012 monoclonal antibody). Error bars represent SEM. D) HBGA BT50 values were calculated using nonlinear fit – one site logIC50 curve equations with top and bottom constraints 0 and 100, respectively. Values for 95% confidence intervals are reported in parentheses.

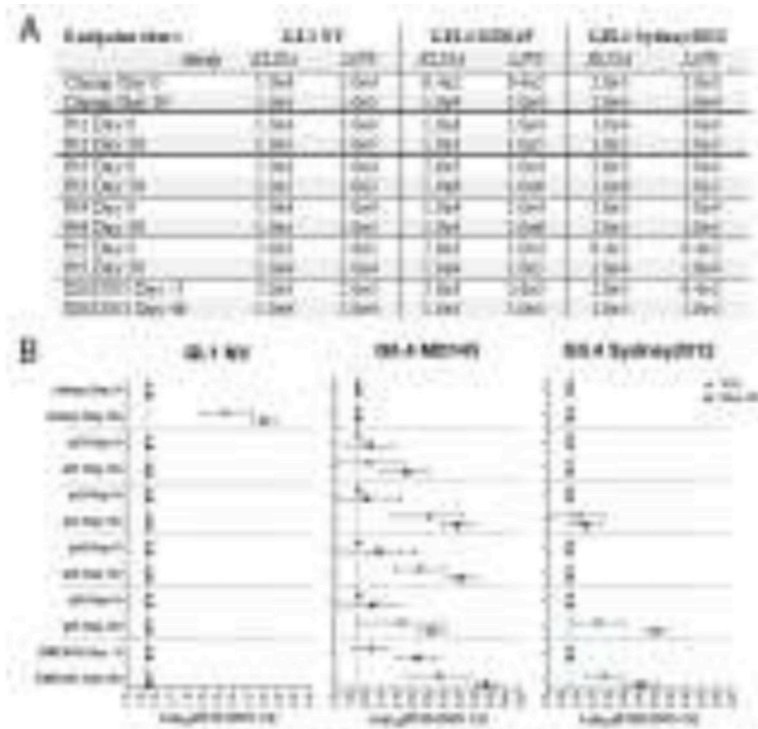


Fig 5. Changes in anti-HuNoV and HBGA blocking antibody titers were detected in complex sera using VLPs and Rluc-VP1 antigens. Serially diluted patient sera collected pre-and post- challenge/infection were preincubated with GI.1 NV, GII.4 MD145, and GII.4 Sydney2012 VLPs and Rluc-VP1 proteins. Antigen-antibody mixtures were then applied to plates coated with either protein A/G (A) or PGM (B) to determine HuNoV recognizing antibody titer and HBGA blocking antibody titer, respectively. A) Average O.D. and RLU were determined and plotted relative to negative, pre-immune-treated controls. Cutoff values were calculated based off negative control readings plus three standard deviations. Reported titers are the last positive serum dilution above this negative control cutoff. B) Graphs report BT50 values of HBGA blockade curves generated using the nonlinear fit – one site logIC50 analysis. Lowest serum dilution (1:80) is represented by the dashed vertical line. Bars represent 95% confidence intervals of BT50s.

Table 1.

Gateway forward and reverse primers used to generate HuNoV Rluc-VP1 constructs.

NoV strain	Accession No.	VP1 forward primer	VP1 reverse primer
Hu/NoV/GI.1/ Norwalk/ 1968/US	M87661	5' <u>GGGGACAAGTTTGTACAAAAAAGCAGGCTTA</u> ^a ATGATGATGGCGTCTAAGGACG 3'	5' <u>GGGGACCAC</u> TCGGCGCAGAC
Hu/NoV/GII.4/ MD14512/1987/ US Hu/NoV/GII.4/ Sydney/ NSW0514/2012/ AU	AY032605 JX459908.1	5' <u>GGGGACAAGTTTGTACAAAAAAGCAGGCTTC-ACC</u> ^a ATGAAGATGGCGTCGAATGACG 3'	5' <u>GGGGACCAC</u> TTA ^b TAATGCA ACGCC 3'
Mu/NoV/GV/ MNV1/2 002/USA	AY228235.2	5' <u>GGGGACAAGTTTGTACAAAAAAGCAGGCTTCACC</u> ^a ATGAGGATGAGCGACGGCGCAGCGCCAAAAGCC 3'	5' <u>GGGGACCAC</u> TTGTTTGAGCA

^a *attB1* sites are underlined,^b STOP codons are in bold

Table 2.

Highest endpoint titers of animal hyperimmune sera evaluated by ELISA (VLPs) or LIPS (Rluc-VP1)

Test sera *	Antigen					
	GI.1 NV		GI.4 MD145		GI.4 Sydney2012	
	<i>ELISA</i>	<i>LIPS</i>	<i>ELISA</i>	<i>LIPS</i>	<i>ELISA</i>	<i>LIPS</i>
NV GP sera	1.0e4	1.0e4	<160	<160	<160	<160
NV RB sera	1.0e5	1.0e5	2.5e3	2.5e3	2.5e3	1.0e4
MD145 GP sera	1.0e4	1.0e4	1.0e5	1.0e5	1.0e5	1.0e6
MD145 RB sera	1.0e4	1.0e4	1.0e5	1.0e5	1.0e4	1.0e5

* Assays were performed in duplicate and values were averaged as described in text to determine the highest serum dilution that resulted in O.D. (for ELISA) and RLU values (for LIPS) of the negative control sera + 3 standard deviations